RiESTech
Recent in Engineering Science and Technology

MBI

Article

Surface Character of Magnetic Ce-Doped TiO_2 for Photocatalytic Performance Enhancement

Tia Rahmiati [1]*, Ching-Cheng Chen [2], Asmahani Saad [3], Nugroho Eko Setijogiarto [1], Asep Apriana [1]

[1] Department of Mechanical Engineering, Politeknik Negeri Jakarta, Depok 16424, Indonesia
[2] Department of Materials Science and Engineering, National Dong Hwa University, Hualien 97401, Taiwan
[3] Department of Civil Engineering , International Islamic University Malaysia, Kuala Lumpur 50728, Malaysia
* Correspondence: tia.rahmiati@mesin.pnj.ac.id

Abstract: Using a modified sol-gel method for magnetic photocatalyst, the core shell structure of Ce-doped TiO_2@SiO_2@ferrite composite nanoparticles (NPs) was created. X-ray diffraction (XRD), Brunauer–Emmit–Teller (BET), and a superconducting quantum interference device (SQUID) were used to examine the physicochemical properties of the products as they were prepared. The ultraviolet-visible spectrometry (UV-vis) was used to measure the catalyst's photocatalytic activity. On the composite NPs' outer shell coating, the anatase phase related to the TiO_2 structure was constructed. On the Ce-doped TiO_2 layers, a mesoporous structure with uniform pore size was created, resulting in a specific surface area of 111.916 m^2g^{-1}. In the meantime, the thin TiO_2 coating contained the redox couple of Ce^{3+} and Ce^{4+}. An external magnetic field can also be used to separate the catalyst's magnetic NPs from the reaction system. In the aqueous solution of methylene blue (MB), the degradation efficiency and product performance were both 50 percent.

Keywords: Magnetic photocatalyst; Photodegradation; Cerium doped TiO_2; Core shell structure

Citation: Rahmiati, T., Chen, C.-C., Saad, S. A., Eko, N., & Apriana, A. (2023). Surface Character of Magnetic Ce-doped TiO2 for Photocatalytic Performance Enhancement. Recent in Engineering Science and Technology, 1(01), 1–6. https://doi.org/10.59511/riestech.v1i01.2

Academic Editor: Iwan Susanto

Received: 17 October 2022
Accepted: 18 November 2022
Published: 1 January 2023

1. Introduction

Organic contaminants and energy crises have been creating serious threats to the environment as globalization and industrialization progress [1, 2]. Semiconductor photocatalysts are a tried-and-true method for converting solar energy into chemical energy to break down pollutants, especially in liquid waste [3, 4]. Due to its excellent photoelectric properties, non-toxic nature, low cost, and high stability, a semiconductor material titanium oxide (TiO_2) has been widely utilized in this system [5–8]. However, the photocatalytic process is hindered in practical applications by the rapid rate of recombination for charge-carrying electron pair holes and the limited range of light response [9, 10]. Numerous attempts have been made to reduce the likelihood of electron hole pair recombination and widen the gap in the TiO_2 absorption band to resolve this issue. Sensitivity design, impurity doping, and integration with other semiconductors are some of the implemented strategies [11–14].

Cerium (Ce) is one of the rare earth elements that has sparked a lot of controversy due to its advantageous properties, which include: 1) the redox couple Ce^{3+}/Ce^{4+}, which facilitates the transfer of photogenerated holes to electron donors, and 2) the straightforward formation of vacancies with a relatively high mobility [15]. Cerium has also been demonstrated to be an effective dopant for increasing the quantum yield in the photocatalytic process by effectively narrowing the band gap and preventing electron-hole recombination [16]. However, the wastewater treatment procedure for separating and manipulating TiO_2 nano composer particles presents yet another issue. Failing to recycle these nanostructures can result in new forms of pollution and also increase the processing costs. Nevertheless, due to their unique magnetic response, chemically modified surface, and low cytotoxicity, the include of nano-based magnetic components of TiO_2 particles as catalyst is of particular interest [17]-[19].

As a potential semiconductor photocatalyst material for the degradation of liquid waste from textile dyes, we modify magnetic nanoparticles (NPs) with Ce-coated TiO_2. With Xe arc lamp simulating irradiation of sunlight the aqueous solution of methylene blue (MB) took a role as a model pollutant to carry out the photocatalytic activity. The atomic of TiO_2 with and without doped Ce were the two experimental parameters investigated. Co-doping Ce's potential mechanisms and synergistic effects were thoroughly discussed.

2. Materials and Experiment Methods

2.1 Catalyst sintesis

The tetrabutly titanate ($Ti(OC4H9)4$) that was used to create the final CTSF model was coated with SiO_2@ferrite (SF) nanoparticles and doped with 0.5 Ce weight percent. The model was calcined for three hours at 500 °C to produce the anatase phase of TiO_2. The sample of F, SF, TSF, and 5CTSF, respectively, were noted for each sample, which included ferrite, SiO_2@ferrite, TiO_2@SiO_2@ferrite, and Ce-TiO_2@SiO_2@ferrite. To determine the photocyatalist performance and surface structure properties, the samples were further analyzed and tested.

2.2 Catalyst characterization

The crystalline structure observed by X-ray diffraction (XRD) with Cu K radiation (= 0.154056 nm) at a scan rate of 3 ^{o}/minutes (Rigaku D/Max-II, Tokyo, Japan). Brunauer–Emmit–Teller (BET) nitrogen adsorption with the Autosorb-1C instrument (Quanta Chrome, Boynton Beach, FL) was used to measure the surface characteristics of surface area, pore volume, and pore size. Adsorbent was nitrogen gas, and the BJH cumulative adsorption method was used to calculate pore volume and size. The superconducting quantum interference device (MPMS5;) was utilized for the ambient temperature measurement of the magnetization properties. With a maximum magnetic field of 10 kOe, the setup (Quantum Design, San Diego, CA) was used.

2.2 Photocatalytic activity

Using a UV–VIS spectrometer (Evolution 220;) and 0.30 g of TSF and 5CTSF magnetic photocatalyst powders in 50 mL of 10 mg/L MB aqueous solution, the concentration of MB was photodegraded. Adsorption–desorption equilibrium prior to the UV illumination process was gained by stirring the suspension for thirty minutes in the darkroom using ultrasonic vibration apparatus. The irradiation function of the TSF and 5CTSF composite was measured under a 35-W Xe arc lamp acting as a simulated sun. Within the duration of six hours, every one hour five milliliters of the suspension were taken, centrifuged, and then analyzed using the MB absorbance intensity at 664.6 nm for powder separation.

3. Results and Discussion

The photocatalyst nanoparticle XRD pattern for the F, SF, and TSF samples is depicted in Figure 1. The XRD pattern of sample F in Figure 2(a) demonstrates the spinel crystal structure of particle ferrite (Ni-Zn). The pattern was consistent with the crystal structure of ferrite Ni-Zn as determined by the Joint Committee of Powder Diffraction Standard (JCPDS), which had the number 08-0234. However, a second phase exist in the pattern, and its JCPDS value was 72-0469 for Fe_2O_3. Additionally, a broader peak pattern suggests that the particles are nanometer sized. The pattern in Figure 1(b) does not contain any SiO_2 peaks after the SiO_2 layer has been deposited. It could be because of the SiO_2 layer's amorphous structure. Some of the new peaks observed in the XDR pattern in

Figure 1(c) can be attributed to the coating of the TiO_2 and Ce-doped TiO_2 on the SF particles. The intensity of some of their previous peaks decreased in tandem with their current one.The anatase phase of TiO_2 gave rise to the new crystal peak at 25.27° in the (101) plane of 2-XRD. The anatase crystal structure of TiO_2 is represented by JCPDS number 21-1272, and the pattern is in line with that. According to the result, the nanoparticle composite of TiO_2@SiO_2@ferrite had a successful TiO_2 layer formed on its outer shell. However, the pattern lacked any Ce peaks, indicating that the entire doping Ce had been incorporated into the TiO_2 crystal structure shown in Figure 2 (b).

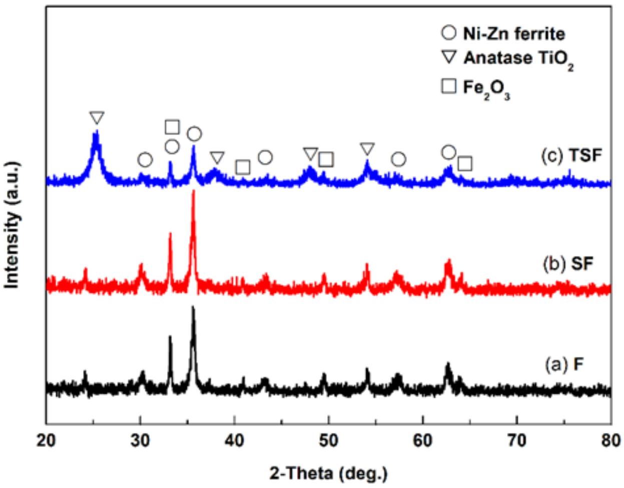

Figure 1. XRD pattern for catalyst particles of (a) F, (b) SF, (c) TSF and (d) 20CTSF

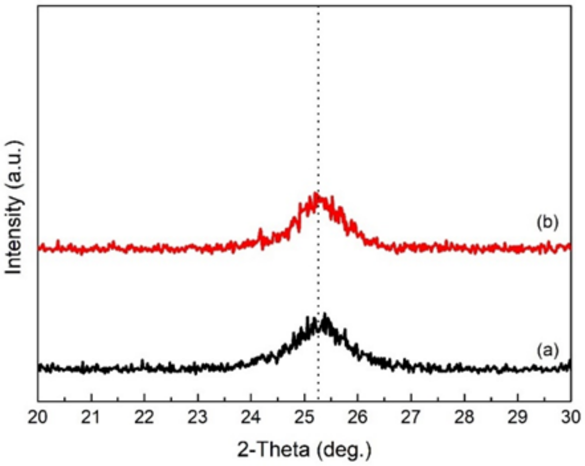

Figure 2. XRD pattern for catalyst particles (a) TSF and (b) 5CTSF between 20 – 30°

The photocatalyst magnetic particles' specific surface area and pore-size distribution were characterized using an adsorption analysis of nitrogen gas. Nitrogen gas isothermal adsorption-desorption for samples F, SF, TSF, and 5CTSF are depicted serially in Figure 3 (a, b, c, and d). For TSF and 5CTSF, the type IV isotherm and H1 type hysteresis loop were investigated, indicating a mesoporous structure of the product. Using the standard multi-points Brunauer-Emmett-Teller (BET) method, the specific surface area (SSA) of the two models was determined to be 126.831 m^2g^{-1} and 135.232 m^2g^{-1}, respectively. However, the SSA values for the F and SF models were lower than those for the other two models, as shown in Table 1. The greater the SSA, the more surface contact area could be made possible, which could help speed up the photocatalyst reaction to reduce dye molecules.

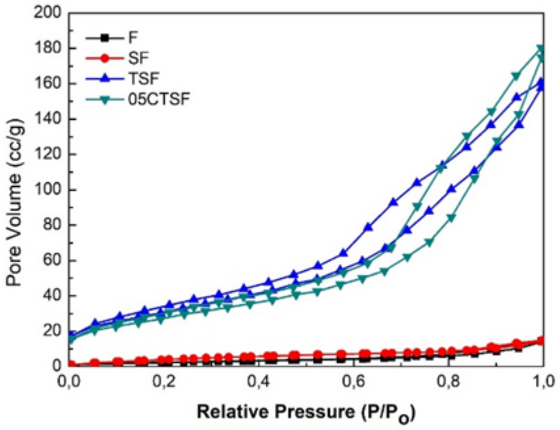

Figure 3. Adsorpsi-desorpsi nitrogen secara isothermal untuk partikel magnetik (a)F, (b) SF, (c) TSF, dan (d) 05CTSF

Table 1. The pore characteristic of photocatalyst nanoparticles

Sample	Surface Area S_{BET} (m^2/g)	Pore Diameter (Å)	Pore Volume (cc/g)
F	7.586	15.949	0.022
SF	7.395	15.902	0.018
TSF	126.831	26.457	0.244
5CTSF	135.232	28.745	0.345

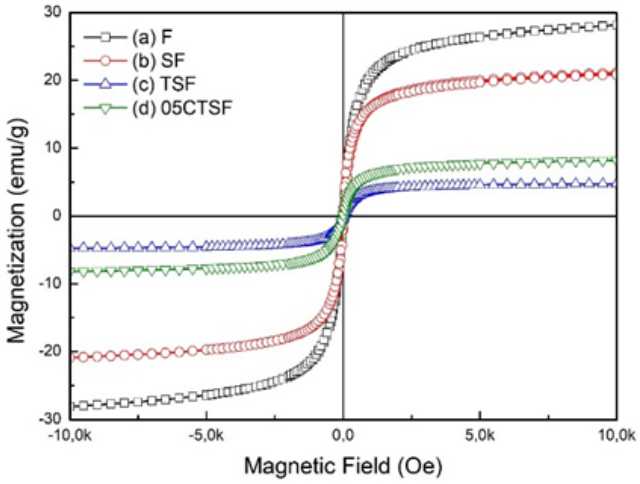

Figure 4. Room-temperature magnetization curve of (a) F, (b) SF, (c) TSF, and 5CTSF composite NPs.

The magnetic curve of magnetic NPs tested at room temperature is shown in Figure 4.F, SF, TSF, and 5CTSF regularly have saturation magnetization values of 28.12, 21.13, 4.73, and 8.25 emu/g, respectively. The value represented the capacity of performance NPs to respond to the magnetic field. The more strong the NPs affected by the magnetic field, the higher the value gained. The minimal hysteresis loop on the magnetization curve of Ni-Zn ferrite indicates a soft magnetic material with a value of 28.12 emu/g, in contrast to the bulk value of 80 emu/g. Additionally, the nonmagnetic TiO_2 and SiO_2 layer coating over Ni-Zn NPs is responsible for the decreasing saturation magnetization of SF TSF and

5CTSF. The thickness of the shell structure that is formed on the composite magnetic NPs probably influences the lower saturation magnetization. Further, using an external magnetic field from the reaction system, the magnetic NPs can be separated in a magnetic field**.**

The degradation of MB dye solution under visible light with a 35-watt Xe arch lamp was used to measure the photocatalytic activity of TSF and 5CTSF NPs, as shown in Figure 5. Adsorption-desorption reactions took place in a dark room for 30 minutes prior to photo-degradation under visible light. For TSF and 5CTSF NPs, decolorization of MB dye reached up to 24% and 27%, respectively. It is commonly known that the large surface area and numerous pores of the catalyst NPs in table 1 will make it easier to absorb the dyes in the MB solution. The photodegradation efficiencies were found to be gradually rise within the reaction time as the TSF and 5CTSF NP catalysts were loaded under visible light. In just six hours, the degradation efficiency of the catalyst NPs of TSF and 5CTSF increased from 45% to 55%. It was hypothesized that the redox couple Ce^{3+}/Ce^{4+} reduced the band gap energy and effective recombination delay of photo-induced charge carriers, resulting in a higher efficiency for the 5CTSF catalyst [15]. It has a useful dopant that increases the quantum yield in the photocatalytic process by enhancing TiO$_2$'s response [16].

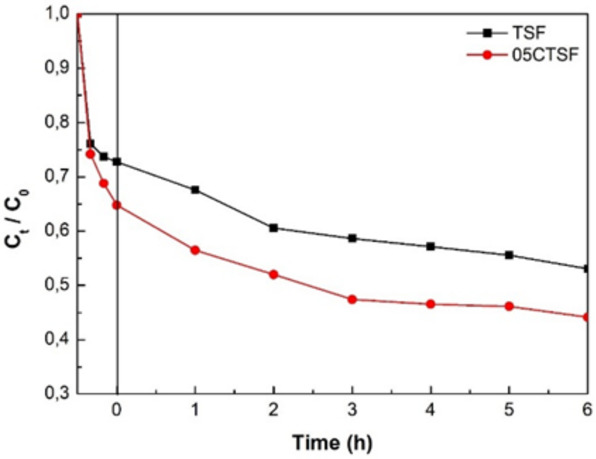

Figure 5. Photodegradation of MB concentration of TSM and 5CTSM NPs composite as a function of irradiation time under visible light, as monitored by changes in the absorbance at 664.6 nm.

4. Conclusions

The magnetic nanoparticles of cerium-doped titanium oxide coated on (Ni-Zn) ferrite NPs as the core were successfully synthesized in this report. On the model's outer core shell structure, the anatase phase of TiO$_2$ structure has formed. The magnetic core shell NPs have increased pore volume while simultaneously increasing surface area. In addition, a sufficient magnetic field may facilitate the separation of catalyst NPs from the reaction system by an external magnetic field. For Ce-doped TiO$_2$, the core shell structure's total degradation efficiency reached up 55% after six hours. For MB dye reduction, the performance of catalys was superior by Ce-doping. The results indicate that the metals transition is one promising option for improving TiO$_2$'s performance and lowering textile limbah's color. To maximize the performance of the photocatalyst for TiO$_2$ NPs, further research was required

Acknowledgments: The authors would like to thank to the research unit and community service of Politeknik Negeri Jakarta for their financial support through the Study Program Leading Research grant in this research.

References

1. J. Lei et al., “Ag/AgCl coated polyacrylonitrile nanofiber membranes: Synthesis and photocatalytic properties,” React. Funct. Polym., vol. 71, no. 11, pp. 1071–1076, 2011.
2. J. Zhang, B. Tian, L. Wang, M. Xing, and J. Lei, Photocatalysis. Singapore: Springer US, 2018.
3. D. V. Bavykin, J. M. Friedrich, and F. C. Walsh, “Protonated titanates and TiO2 nanostructured materials: Synthesis, properties, and applications,” Adv. Mater., vol. 18, no. 21, pp. 2807–2824, 2006.
4. Q. Zhang, D. Q. Lima, I. Lee, F. Zaera, M. Chi, and Y. Yin, “A highly active titanium dioxide based visible-light photocatalyst with nonmetal doping and plasmonic metal decoration,” Angew. Chemie - Int. Ed., vol. 50, no. 31, pp. 7088–7092, 2011.
5. R. Li, H. Kobayashi, J. Guo, and J. Fan, “Visible-light-driven surface reconstruction of mesoporous TiO2: Toward visible-light absorption and enhanced photocatalytic activities,” Chem. Commun., vol. 47, no. 30, pp. 8584–8586, 2011.Title of Site. Available online: URL (accessed on Day Month Year).
6. Y. Zhao, Y. Wang, G. Xiao, and H. Su, “Fabrication of biomaterial/TiO 2 composite photocatalysts for the selective removal of trace environmental pollutants,” Chinese J. Chem. Eng., p. #pagerange#, 2019.
7. Z. Xing et al., Recent advances in floating TiO2-based photocatalysts for environmental application, vol. 225. Elsevier B.V., 2018.
8. Y. Wang et al., “The Application of Nano-TiO2 Photo Semiconductors in Agriculture,” Nanoscale Res. Lett., vol. 11, no. 1, pp. 1–7, 2016.
9. L. L. Tan, S. P. Chai, and A. R. Mohamed, “Synthesis and applications of graphene-based TiO2 photocatalysts,” ChemSusChem, vol. 5, no. 10, pp. 1868–1882, 2012.
10. K. Ozawa et al., “Electron-Hole Recombination Time at TiO2 Single-Crystal Surfaces: Influence of Surface Band Bending,” J. Phys. Chem. Lett., vol. 5, no. 11, pp. 1953–1957, 2014.
11. V. Subramanian, E. E. Wolf, and P. V. Kamat, “Catalysis with TiO2/Gold Nanocomposites. Effect of Metal Particle Size on the Fermi Level Equilibration,” J. Am. Chem. Soc., vol. 126, no. 15, pp. 4943–4950, 2004.
12. F. Chen et al., “Fabrication of Fe3O4@SiO2@TiO2 nanoparticles supported by graphene oxide sheets for the repeated adsorption and photocatalytic degradation of rhodamine B under UV irradiation,” Dalt. Trans., vol. 43, no. 36, pp. 13537–13544, 2014.
13. J. H. Park, S. Kim, and A. J. Bard, “Novel carbon-doped TiO 2 nanotube arrays with high aspect ratios for efficient solar water splitting,” Nano Lett., vol. 6, no. 1, pp. 24–28, 2006.
14. W. L. Ong, M. Gao, and G. W. Ho, “Hybrid organic PVDF-inorganic M-rGO-TiO2 (M = Ag, Pt) nanocomposites for multifunctional volatile organic compound sensing and photocatalytic degradation-H2 production,” Nanoscale, vol. 5, no. 22, pp. 11283–11290, 2013.
15. T. Yu, X. Tan, L. Zhao, Y. Yin, P. Chen, and J. Wei, “Characterization, activity and kinetics of a visible light driven photocatalyst: Cerium and nitrogen co-doped TiO2 nanoparticles,” Chem. Eng. J., vol. 157, no. 1, pp. 86–92, 2010.
16. I. Tbessi et al., “Effect of Ce and Mn co-doping on photocatalytic performance of sol-gel TiO2,” Solid State Sci., vol. 88, pp. 20–28, 2019.
17. C. C. Chen, Y. P. Fu, and S. H. Hu, “Characterizations of TiO2/SiO2/Ni-Cu-Zn Ferrite Composite for Magnetic Photocatalysts,” J. Am. Ceram. Soc., vol. 98, no. 9, pp. 2803–2811, 2015.